Zeitschrift Kunststofftechnik
Journal of Plastics Technology

www.kunststofftech.com · www.plasticseng.com

archivierte, peer-rezensierte Internetzeitschrift
archival, peer-reviewed online Journal of the Scientific Alliance of Plastics Technology

WAK
Scientific Alliance of the University Professors of Plastics Technology

eingereicht/handed in: 09.12.2021
angenommen/accepted: 26.04.2022

J. Schmid[1], D. F. Weißer[1], D. Mayer[1], Prof. Dr.-Ing. habil. L. Kroll[2], Dr.-Ing. S. Müller[2], Prof. Dr.-Ing. R. Stauch[1], Prof. Dr.-Ing. M. H. Deckert[1]
[1] - Esslingen University of Applied Sciences, Faculty of Mechanical and Systems Engineering
[2] - Chemnitz University of Technology, Department of Lightweight Structures and Polymer Technology

Analysis of two different nozzle systems for hot gas welding using CFD simulations and measurement results

With the help of CFD simulations, a nozzle system (top nozzle) for hot gas welding is developed, which encloses the weld seam during heating. The significantly more controlled flow behavior of the hot gas improves the processing window, increases the reproducibility and achieves a significantly more efficient heating time of the polymer weld seam. The CFD simulations used to develop the new nozzle system are validated by temperature measurements in the hot gas welding process with IR camera and thermocouples.

Analyse von zwei verschiedenen Düsensystemen zum Heißgasschweißen mittels CFD-Simulationen und Messergebnissen

Mit Hilfe von CFD-Simulationen wird ein Düsensystem (Aufsatz-Düse) für das Heißgasschweißen entwickelt, welches die Schweißnaht während der Erwärmung umschließt. Durch das wesentlich kontrolliertere Strömungsverhalten des Heißgases wird das Verarbeitungsfenster verbessert, die Reproduzierbarkeit erhöht und eine deutlich effizientere Erwärmungszeit der Kunststoffschweißnaht erreicht. Die zur Entwicklung des neuen Düsensystems verwendete CFD-Simulation wird durch Temperaturmessungen im Heißgasschweißprozess mit IR-Kamera und Thermoelementen validiert.

Analysis of two different nozzle systems for hot gas welding using CFD simulations and measurement results

J. Schmid, D. F. Weißer, D. Mayer, L. Kroll, S. Müller, R. Stauch,
M. H. Deckert

1 THE HOT GAS WELDING PROCESS

To join technical polymer components, both non-contact welding processes, such as infrared [1-4] and laser welding [5, 6], and contacting processes, such as vibration [7, 8] and ultrasonic welding, have been established in series production [9]. However, joining processes that melt the thermoplastic without contact, e.g. by radiation or convection heating, have been increasingly investigated and developed in recent years [1-4, 10, 11]. The reason for this is the formation of particles in friction or vibration welding or the adhesion of plastic melt in hot plate welding. The heating of components that is not free of particles is increasingly a criterion for exclusion when selecting a suitable joining process for engineering polymers [12, 13].

Hot gas welding is a further development of the widely used hot plate welding [14-19]. The advantage of hot gas welding is not only the non-contact heating but it is also the free design of the weld seam. In contrast to the usual welding processes such as ultrasonic or vibration welding, three-dimensional weld seams can be produced comparatively easily [20-22]. The disadvantages of the process are the highly complex tools, relatively long cycle times and the high-energy consumption [22, 23]. In recent years, various studies are carried out on hot gas welding. [9] gives an overview about the process and the influence of the process parameters e.g. heating time, joining path, joining pressure and process gas. Nitrogen is usually used as process gas [9, 22]. The influence of compressed air as process gas for hot gas welding is being investigated in [9, 24]. A further development of the nozzle system is shown in [20, 23, 25-29]. Recently, immersion nozzle systems [20, 23, 25-28] and slot nozzle systems [23, 27, 29] for hot gas welding are investigated and some of them are already in use.

For hot gas welding, the complete welding contour of both halves of the component to be joined is reproduced with small, closely spaced tubes on the so-called hot gas tool. The hot gas flow coming out of the tubes of the hot gas tool melts the polymer at the joining surfaces. Subsequently, the components are joined under pressure, Figure 1. Today hot gas welding processes often show limited processing windows and are therefore difficult to adjust and control. The currently used conventional "round nozzle" creates an impingement flow which

heats the joining zone of the component only selectively and creates a crater-like structure [23, 27]. This type of nozzle produces comparatively high heat losses and the surface temperatures are difficult to control. The round nozzle system has long heating times because the hot gas flows uncontrollably away from the polymer surface after impinging it [25, 26].

The newly developed “top nozzle” design overcomes the mentioned drawbacks. With this next generation nozzle design the weld joint is entirely covered by the nozzle itself. As a result, the heat loss is minimized and the flow of the hot gas can be controlled much better. For polyamides with different base polymers and different glass fiber contents, an average reduction in heating time of 50 % is possible. In exceptional cases, a reduction of 60 % can be achieved. The achieved weld strengths for the tested materials are comparable or higher with the top nozzle system. [25, 26]

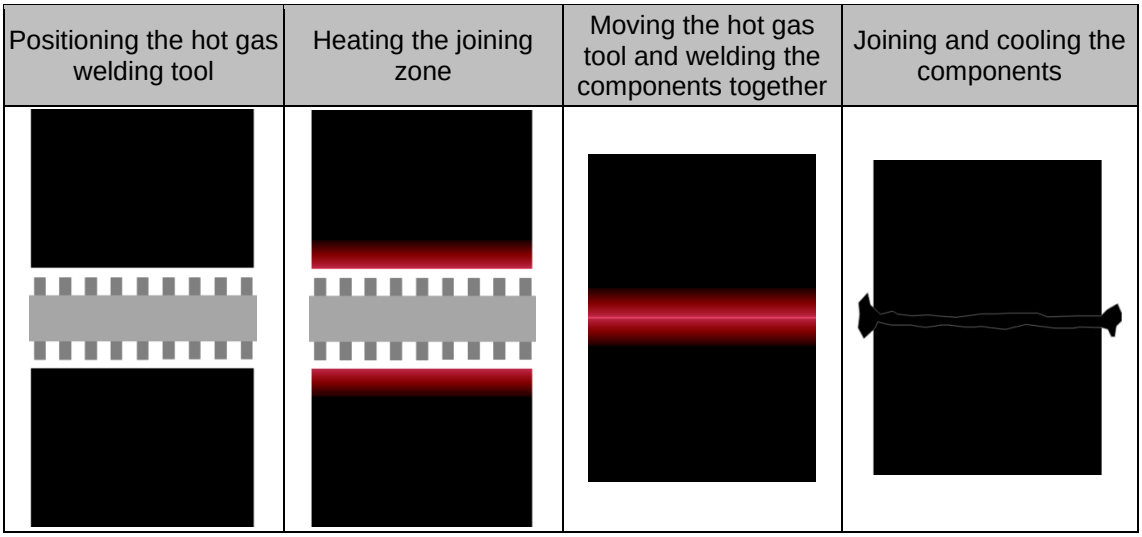

Figure 1: Hot gas welding sequences

2 THEORY OF IMPINGMENT FLOW

For the following description of the theory of impingement flow from round and slot nozzles, it is assumed that the fluid flowing out of the nozzle is the same fluid as the surrounding area. The flow field between the nozzle and the solid can be divided into three different regions (sections). As can be seen in Figure 2, a free jet is formed directly after the nozzle exit. This free jet is broadened and slowed down by the interaction with the surrounding fluid. The free jet changes into a stagnation flow at a certain distance from the solid [30].

In the area where the jet is affected by the wall (stagnation area), the wall-normal component of the velocity decreases to zero, while the wall-parallel component increases from zero to a maximum value at a certain distance from

the stagnation point. At the stagnation point the velocity is zero. The wall jet (downstream zone), as well as the free jet, increases in jet thickness due to mixing with the ambient fluid and therefore the velocity of the hot gas decreases. At a distance of one to two nozzle diameters from the center point of the nozzle the maximum of the wall-parallel velocity can be detected [30].

Schabel and Martin study single round nozzles and two-dimensional nozzle arrays (x- and y-direction) [30]. In the hot gas welding process studied in this paper, only one-dimensional nozzle arrays (x- or y-direction) are used.

The Reynolds number for the simulations carried out is calculated according to (1), (2) and ranges from Re = 275 to 584 in the studied areas. Hereby describes c_F the flow velocity of the hot nitrogen, d the hydraulic diameter of the single tube (1.7 mm) and ν the kinematic viscosity of nitrogen in the investigated temperature range (290 °C to 365 °C). The kinematic viscosity of nitrogen with respect of the gas temperature is taken from [30] and interpolated accordingly.

$$\mathrm{Re} = \frac{c_F \cdot d}{\nu_{365\,°C}} = \frac{9.69\,\frac{m}{s} \cdot 1.7 \cdot 10^{-3}\,m}{60 \cdot 10^{-6}\ \ m^2/s} = 275 \tag{1}$$

$$\mathrm{Re} = \frac{c_F \cdot d}{\nu_{290\,°C}} = \frac{16.15\,\frac{m}{s} \cdot 1.7 \cdot 10^{-3}\,m}{47 \cdot 10^{-6}\ \ m^2/s} = 584 \tag{2}$$

The range of validity of the Reynolds number for the calculation of the Nusselt number for the impingement flow for a single circular nozzle or a circular nozzle array specified in [30] is Re > 2000, Table 1. The hot gas welding process lies beyond this validity limits mentioned in [30] with respect to the Reynolds number and the geometrical dimensions.

Validity limits from [30]	Hot gas welding process
$2{,}5 \leq \frac{r}{D} \leq 7{,}5$	$\frac{r}{D} = \frac{2.0\ mm}{1.7\ mm} = 1.2$
$2{,}0 \leq \frac{H}{D} \leq 12$	$\frac{H}{D} = \frac{2.0 \text{ to } 6.0\ mm}{1.7 \text{ to } 4.0\ mm} = 1.2 \text{ to } 3.5$
$2000 \leq \mathrm{Re} \leq 400.000$	$\mathrm{Re} = 275 \text{ to } 584$

Table 1: Comparison of the Reynolds number and geometrical dimensions according to [30]

For these two reasons, it is not possible to rely on existing knowledge and a CFD analysis of the existing flow problem is necessary. Furthermore, the reduction of the calculation of the Nusselt number from the two-dimensional array of [30] to the case of one-dimensional nozzle field studied here is not straightforward.

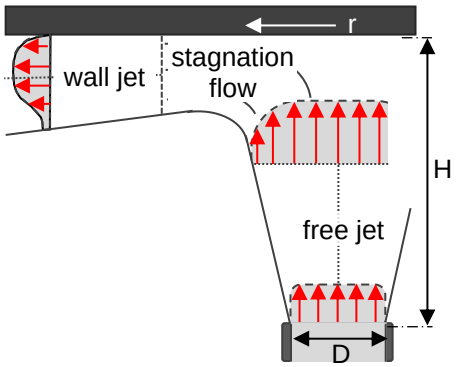

Figure 2: Impingement flow from a slot or round nozzle [30]

3 STRUCTURE OF THE CFD SIMULATION MODEL

To perform the CFD simulations, the CFD software “Simcenter STAR-CCM+ 2020.1” is used. The simulation model of the round nozzle, Figure 3 (left), consists of four tubes (fluid), polymer (solid) and the free flow area. The new top nozzle, Figure 3 (right), consists of four tubes with top nozzle (fluid), polymer (solid) and the free flow area. The individual tubes have an inner diameter of d_{inside} = 1.7 mm ($d_{outside}$ = 2.0 mm) and a distance of Δx = 3.3 mm. The model is symmetric at the front and at the back (symmetry plane - blue area in Figure 3) to simulate an infinitely long weld. The simulation is limited to heat transfer by convection. Superimposed heat transfer by radiation is very low due to the low visibility factor between the tube and the polymer and can therefore be neglected.

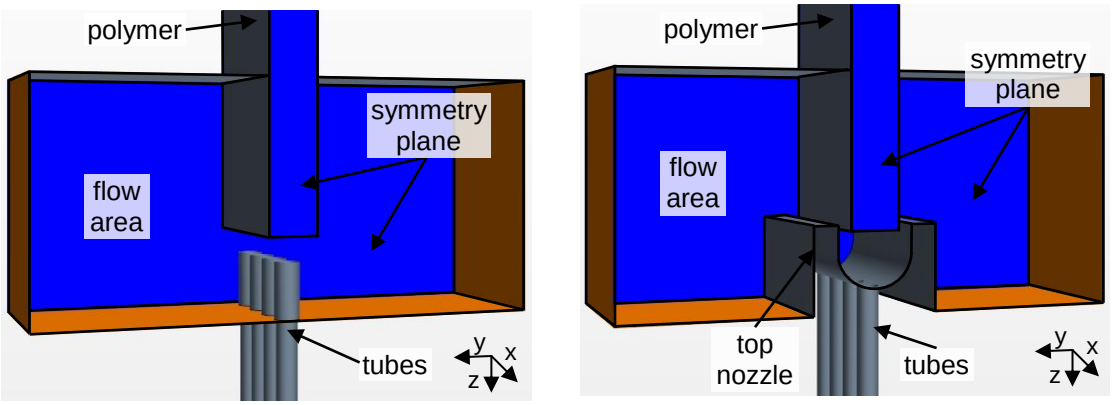

Figure 3: Illustration of the simulation models of the round nozzle (left) and the simulation model of the top nozzle (right)

The simulation process contains the following steps:

- Creation of the computational mesh
- Calculation of the steady-state flow without heat transfer processes in the polymer (→ initial flow field for transient simulation)
- Enabling the heat transfer in the simulation model
- Transient simulation of the heating of the polymer for the physical simulation time

Properties of the CFD model:

- Laminar flow
- Calculation of the gas (nitrogen) properties
    - Polynomial density and specific heat (temperature dependent)
    - Dynamic viscosity (temperature dependent)
    - Thermal conductivity (temperature dependent)
- Calculation of the polymer (PA6-GF40 and PA66-GF35) properties
    - Polynomial density and specific heat (temperature dependent)
    - Thermal conductivity (temperature dependent)
- Polyhedral cells: 5.4 million (round nozzle); 5.1 million (top nozzle)
- Physical time: 25.0 s (round nozzle); 12.5 s (top nozzle)
- Time step = 0.01 s

According to [31], an impingement flow is considered turbulent if the Reynolds number is larger than 2000 (Re > 2000). The investigation of the Nusselt number in [31] shows that impingement flows for Re < 2000 and a nozzle-to-plate-spacing of H/D < 5.5 are laminar. According to Simionescu [32], impingement flows are fully laminar between Re = 300 to 1000. Depending on the process parameters, Reynolds numbers between 275 and 584 and nozzle-to-plate-spacings between 1.2 and 3.5 appear for the hot gas welding process (see Table 1). Due to low Reynolds numbers and the low nozzle-to-plate-spacings laminar CFD simulations are performed.

In the region of interest for the heat transfer of the welding process the predominantly laminar character of the hot gas flow can be seen in Figure 4.

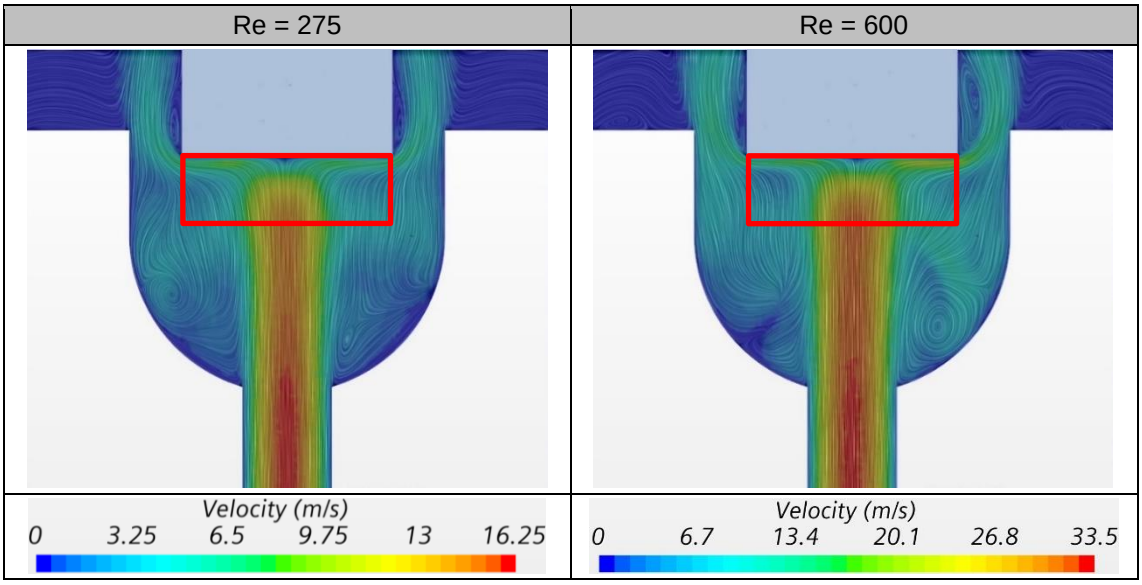

Figure 4: Flow field of the investigated hot gas welding process

4 VALIDATION OF THE SIMULATION RESULTS

To validate the simulation results, temperature measurements are performed during the welding process with an infrared camera system (IR) and additionally with disposable thermocouples. The validation of the simulation is done by temperature measurements under variation of the nozzle system and the materials. Furthermore, the melting behavior of the polymer of the round and of the top nozzle system is validated.

4.1 Test setup for validation of the simulation

To analyze the heating of the polymer, temperature measurements are performed during the welding process with the round and the top nozzle. The hot gas welding system (type: VDP 2012, manufacturer: KVT Bielefeld GmbH, Bielefeld) is equipped with pressure sensors and an IR camera system, Figure 5 right. Nitrogen is used as process gas to heat and melt the polymer. The temperatures during heating of the polymer are measured with thermocouples type J. For this purpose, holes (Ø 0.5 mm) are made at the corresponding points with a suitable CNC milling machine. Eight measuring points are provided per plate, Figure 5 left. A thermocouple is applied to the polymer surface to determine the polymer surface temperature (0.0 mm (P)). Another thermocouple is positioned at a distance of 0.1 mm from the polymer surface to measure the gas temperature next to the polymer surface (+ 0.1 mm (G)). The other six thermocouples are placed 0.5 mm below the polymer surface (- 0.5 mm (P)) with a distance of 3.3 mm.

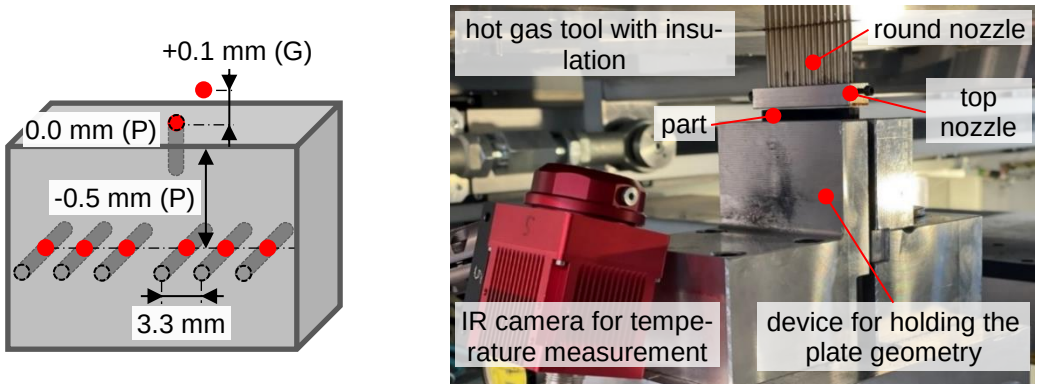

Figure 5: Measuring points in the left half of the polymer plate (dark grey: polymer plate, red; measuring points), left; test setup, right.
+ 0.1 mm (G), gas temperature on polymer surface; 0.0 mm (P), temperature of polymer surface; - 0.5 mm (P), temperature of polymer in 0.5 mm depth

4.2 Investigated materials

The investigations in this work are limited to polyamides, since these are mainly used for technical components in the industrial environment. Polyamides are semi-crystalline engineering thermoplastics. PA6 and PA66 are represented by the same chemical formula $(C_6H_{11}ON)_n$. The two polyamides differ in their structural composition. The higher melting point and lower water absorption of PA66 can be explained by the different molecular structure [33]. Due to the higher solidification temperature and shorter crystallization time, PA66 has a very short cycle time compared to PA6. The rapid solidification of the PA66 melt is a disadvantage in combination with glass-fiber-reinforced grades, because poorer surface quality and distortion of the components are to be expected [33].

The mechanical properties of glass fiber-reinforced PA6 and PA66 are at the same level for freshly molded resin. Due to the lower water absorption with the exception of the toughness value, the mechanical properties of conditioned PA66 are at a slightly higher level compared to conditioned PA6. If the glass fiber content of PA6 is increased by 5 %, the mechanical properties in the conditioned state are at the same level [33].

To have almost the same level of mechanical properties but different base polymers, the investigations are carried out with the following polyamides. Both of these materials are widely used on the market and have a great technical relevance. PA6-GF40 has an approximately 40 K lower melting point than PA66-GF35, Table 2:

- PA6-GF40 (Zytel® 73G40HSLA BK416LM, DuPont)
- PA66-GF35 (Zytel® 70G35HSLR BK416LM, DuPont).

Name	Fracture stress	Young's modulus	Melting temperature	Glass transition temperature
PA6-GF40	215 MPa (dry)	13000 MPa (dry)	220 °C (10 °C/min)	70 °C (10 °C/min)
PA66-GF35	210 MPa (dry)	11000 MPa (dry)	263 °C (10 °C/min)	70 °C (10 °C/min)

Table 2: Comparison of selected properties of PA6-GF40 and PA66-GF35

4.3 Validation of the simulated shape of the molten resin

Differences in the melting evolution caused by the round nozzle and the top nozzle are investigated using a PA66-GF35 and compared with the simulation. For this purpose, thin sections of the specimen (micrographs through the weld, transmitted light microscopy) heated by the round nozzle and the top nozzle system are created (weld width 4 mm). The simulations for the round nozzle and the top nozzle show a melting evolution comparable to that of the thin sections.

The different heating behavior of the two nozzle systems can be seen in the cross section of the polymer below the nozzle opening. With the conventional round nozzle, the melting zone of the polymer is shaped convexly and only a few amounts of polymer is melted at the edges of the weld seam, Figure 6. The melting zone is identified by local temperatures above the melting temperature of 260 °C. In contrast, the top nozzle melts the polymer concavely, Figure 7, as it is known from hot plate or IR welding [2-4]. The simulation results, Figure 6 and Figure 7, left and the experimental results, Figure 6 and Figure 7, right show comparable shapes of the melting zone. With the top nozzle, a deeper melting at the edges of the weld seam is evident. This behavior can be explained by the enclosing of the weld seam with the top nozzle.

$T_{hot\ gas\ tool}$	T_{gas}	Process gas	t_{heat}	Nozzle type
475 °C	355 °C	nitrogen	25 s	round

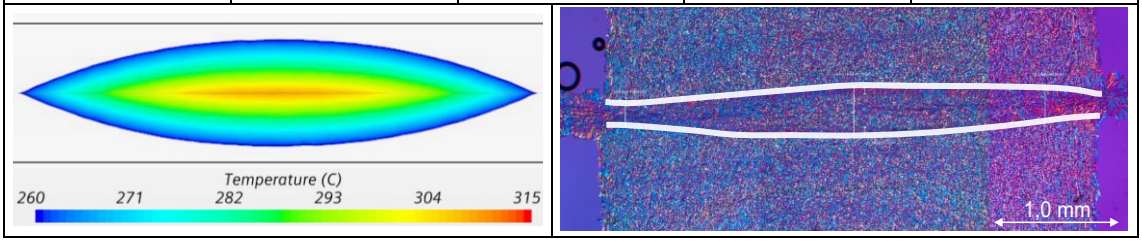

Figure 6: Simulation (left) and thin section image (right, white line) of a weld heated with the round nozzle

$T_{hot\ gas\ tool}$	T_{gas}	Process gas	t_{heat}	Nozzle type
475 °C	355 °C	nitrogen	10 s	top

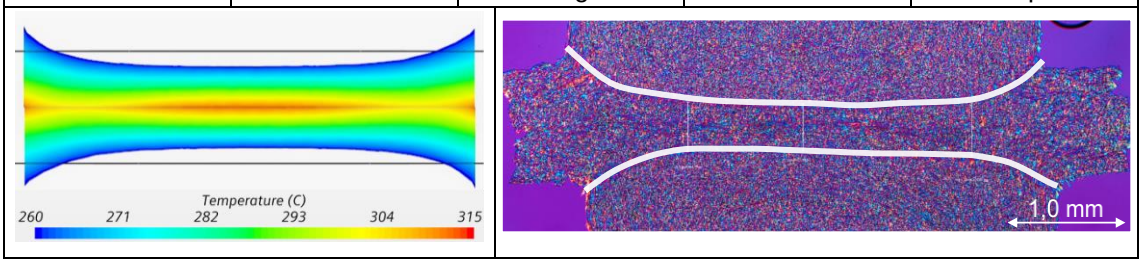

Figure 7: Simulation (left) and thin section image (right, white line) of a weld heated with the top nozzle

4.4 Validation of the simulated transient heating behavior

To validate the simulation, the temperature evolutions on the surface and in the polymer are investigated during the welding process. The gas temperature applied to the polymer is measured with thermocouples. The polymer surface temperature is determined using thermocouples and an IR camera system. The temperatures arising in the polymer at a depth of 0.5 mm are determined using thermocouples. The validation of the simulated transient heating behavior is performed for the round and the top nozzle. The main focus of the simulations carried out is to investigate the behavior of the top nozzle with a 4 mm weld width.

The simulation results in the case of the round nozzle of the gas temperature (+ 0.1 mm (G)) and the temperature of the polymer (PA66-GF35) on the surface (0.0 mm (P)) can be compared with the temperatures measured during the process, Figure 8. It is assumed that the thermocouples which measure the gas temperature need a certain time to be heated by the hot gas (0 to 5 s). This thermal inertia leads to a delayed heat up of the measured temperature values compared to the simulation results in the first five seconds of the process. After five seconds, the influence of the thermal inertia decreases significantly. The effect of thermal inertia is significant when measuring the gas temperature, since the heat transfer between the gas and the thermocouple (gas/solid) is significantly lower than the heat transfer between the thermocouple and the polymer (solid/solid). This effect can be neglected, since the first five seconds of the heating phase are not relevant for the investigations. The temperature predictions after 10 to 25 s are clearly more relevant for the investigations, as these influence the welding result. The temperatures measured at a depth of 0.5 mm (- 0.5 mm (P)) are lower than those calculated in the simulation. It is also assumed that the thermocouples must be heated and thus cool the polymer. The surface temperature measured with the IR camera matches with the simulation results and the temperature measurements with the thermocouples at t = 25 s quite well.

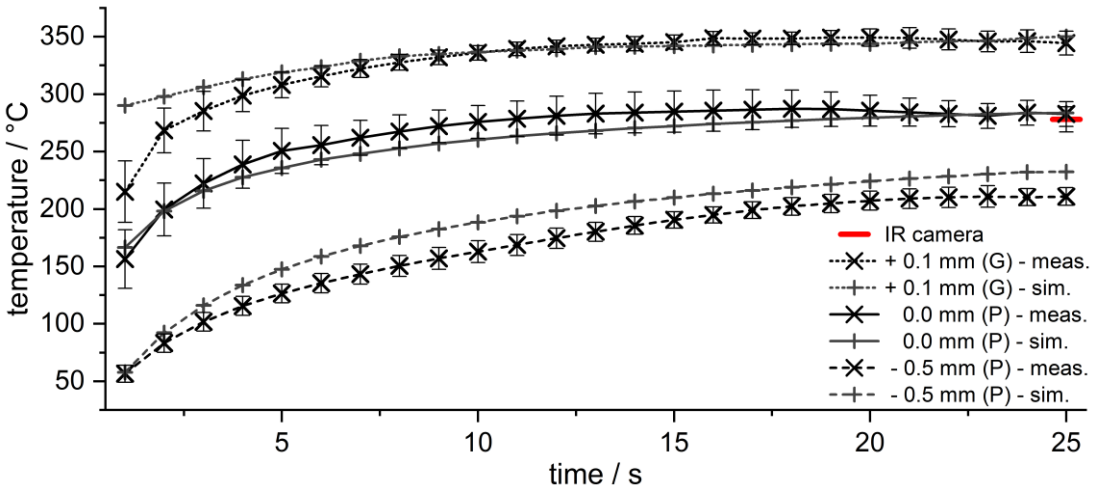

Figure 8: Comparison of temperature measurements and simulation results in the case of the round nozzle at a gas temperature of 355 °C and 1.11 l/min / tube nitrogen as process gas on a PA66-GF35

In the case of the top nozzle, the simulation results of the gas temperature (+ 0.1 mm (G)) and the temperature of the polymer (PA66-GF35) on the surface (0.0 mm (P)) can be compared with the temperatures measured during the process, Figure 9. Here it is also assumed that the thermocouples need a certain time to be heated by the hot gas. The reason for this is similar to Figure 8. The surface temperatures measured with the IR camera measured at t = 12.5 s and the temperatures measured at a depth of 0.5 mm (- 0.5 mm (P)) are slightly lower than those in the simulation calculated, but are within the standard deviation of the measurements.

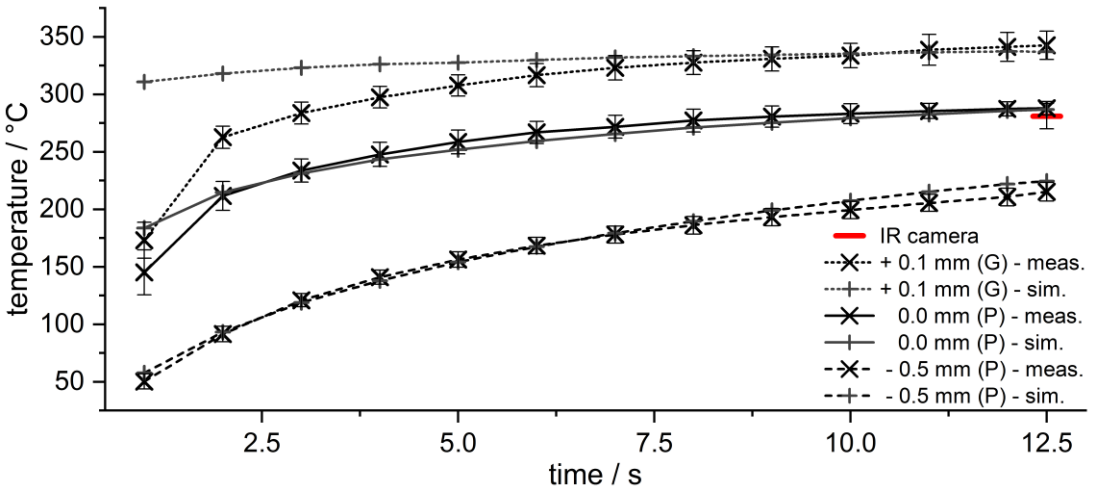

Figure 9: Comparison of temperature measurements and simulation results in the case of the top nozzle at a gas temperature of 355 °C and 1.67 l/min / tube nitrogen as process gas on a PA66-GF35

The simulation and the temperature measurements are additionally performed for the polymer PA6-GF40. It is useful to validate the simulation for polyamides with different base polymers and different glass fiber contents because both investigated materials are frequently used in the automotive industry. For this reason, it makes sense to simulate and validate engineering polymers, as the two polyamides PA6 and PA66 are used in technical components. The further validation is performed for the case of the top nozzle as this nozzle system shows the superior heating and welding performance (see section 5).

The simulation results at a gas temperature of 300 °C are comparable with the temperatures measured during the welding process, Figure 10. The simulated temperatures at a depth of 0.5 mm (- 0.5 mm (P)) match with the temperature measurements of the thermocouples. The surface temperature measured with the thermocouples and the IR camera are slightly higher than the simulated temperature, but are within the standard deviation of the measurements. Here it is also assumed that the thermocouples need a certain time to be heated by the hot gas. The reason for this is similar to the measurements showed in Figure 8 and Figure 9.

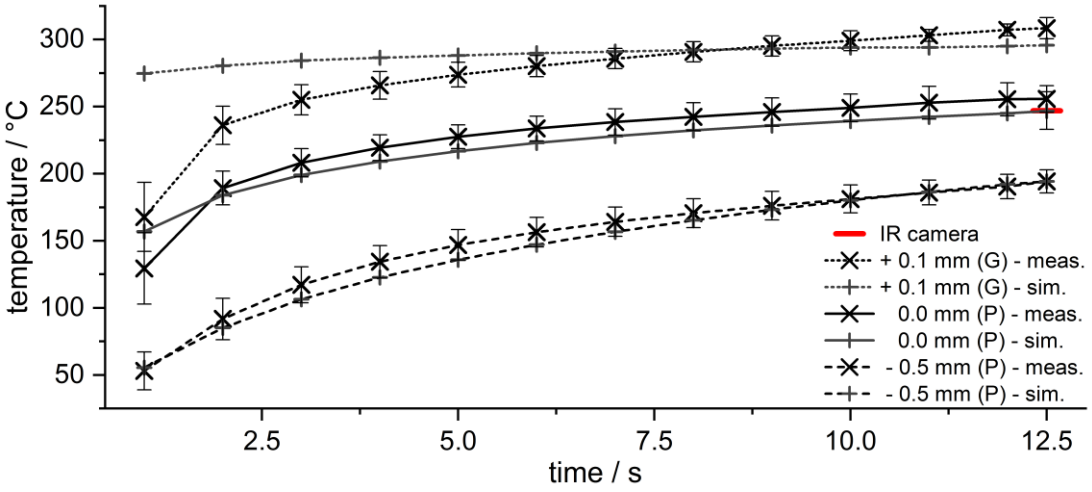

Figure 10: Comparison of temperature measurements and simulation results in the case of the top nozzle at a gas temperature of 300 °C and 1.67 l/min / tube nitrogen as process gas on a PA6-GF40

5 COMPARISON OF THE NOZZLE SYSTEMS

This chapter compares the round and the top nozzle system. It gives a more detailed insight to the differences between the nozzle systems. The new nozzle system for hot gas welding is developed with the help of CFD simulations and can reduce the heating time of the polymer by 50 %. The disadvantageously long melting time of the round nozzle system can be considerably reduced by a modification of the hot gas tool [25]. The main reason for the superior perfor-

mance of this new nozzle system is that the hot process gas is kept in the area next to the surfaces to be joined [26].

The comparison between the round and the top nozzle system is carried out using analogous simulation models. Only the simulated geometry and two process parameters are changed in the simulations:

- round nozzle: 1.11 l/min (volume flow); 25.0 s (heating time)
- top nozzle: 1.67 l/min (volume flow); 12.5 s (heating time).

As seen in Figure 11 (left), according to the round nozzle system the gas impinges on the polymer surface and immediately flows off to the side. The local concentrated heat input leads to stronger overheating in the center of the polymer weld seam, while the edge areas are heated comparatively less. The inhomogeneous melting of the polymer results in a limited joining distance and a narrow process window [25, 26]. The round nozzle system (gas outlet) has a distance of 2.0 mm to the polymer surface. The top nozzle system (gas outlet), Figure 11 (right), has a distance of 4.5 mm to the polymer surface. The new top nozzle encloses the polymer which is covered by 0.5 mm by the nozzle. Due to this difference between the two nozzle systems, the flow field differs significantly. Due to the differing flow field the heating and melting of the edge areas and of the center of the polymer is more homogeneous [28, 34], see also Table 3. Furthermore, it leads to a more homogeneous temperature distribution in the polymer in the case of the top nozzle, see also Figure 11. It must also be taken into account that the flow velocity with the top nozzle is 1.5 times higher in comparison to the round nozzle. The operating parameters such as volume flow and heating time are not the same for the two nozzle systems in a near-series process. The process parameters are adapted to the nozzle systems in such a way that good welding results are achieved in each case (series like process parameters).

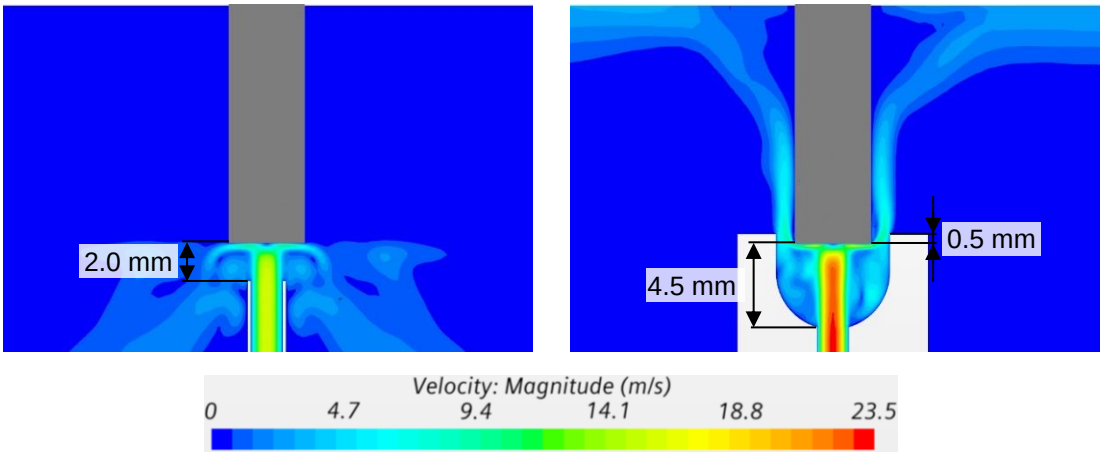

Figure 11: The developing impingement flow in the case of the round nozzle system (left – heating time 25.0 s) and of the top nozzle system (right – heating time 12.5 s)

The difference between the two nozzle systems can also be seen in the temperature field of the polymer surface, Figure 12. In the case of the round nozzle, stagnation points with a steep temperature gradient occur directly below the nozzle openings. This leads to crater like structures on the polymer surface, and the edge areas are heated less intensively. In the case of the top nozzle, the temperature gradient is reduced below the nozzle opening, see also Table 3. In addition, the edge areas are heated much better by the top nozzle compared to the round nozzle and a more homogeneous temperature distribution can be observed.

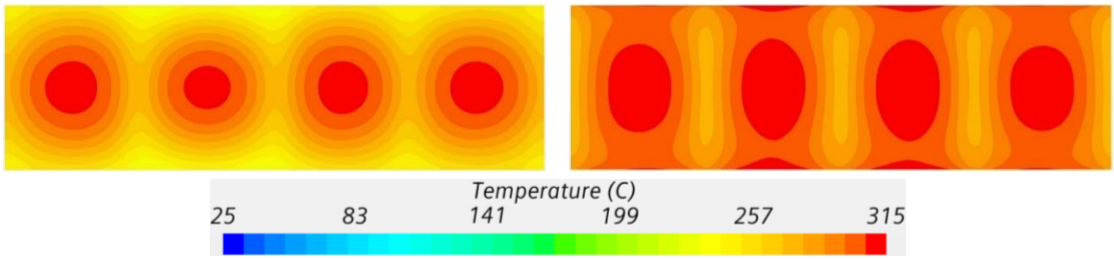

Figure 12: Temperature profiles on the polymer surface in the case of the round nozzle (left – heating time 25.0 s) and of the top nozzle (right – heating time 12.5 s)

The heating in the center of the polymer is comparable for both nozzle systems. The round nozzle heats the polymer convexly, which leads to a low heating at the edge areas, especially beside the nozzle openings, left and right edge in Figure 13, top. The joining path is limited by this inhomogeneous heating of the round nozzle system [25]. The top nozzle heats the polymer concavely by enclosing it and thus leads to more homogeneous heating and melting of the polymer (left and right edge in Figure 13, bottom). The more homogeneous melting by the top nozzle system enables a wider process window and joining path [25].

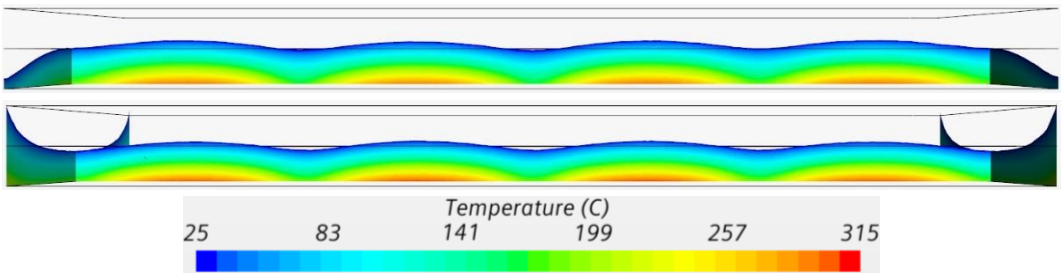

Figure 13: Temperature distributions in the polymer in the case of the round nozzle (top – heating time 25.0 s) and of the top nozzle (below – heating time 12.5 s). (The horizontal lines have a spacing of 0.5 mm.)

The comparison of the simulated temperatures at the end of the heating process shows that the top nozzle heats the polymer by 14 K more on average even when the heating time is reduced by 50 %. Hereby, the resulting temperatures are higher on the surface as well as in a depth of 0.5 mm (T 0.5 mm) inside the polymer. The temperature range is significantly higher with the round nozzle compared to the top nozzle.

Nozzle type	Gas temperature	$\dot{V}$/nozzle	t_{heat}	T 0.0 mm	ΔT 0.0 mm	T 0.5 mm	ΔT 0.5 mm
round	365 °C	1.11 l/min	25.0 s	280 °C	81 °C	222 °C	90 °C
top	365 °C	1.67 l/min	12.5 s	295 °C	41 °C	242 °C	64 °C

Table 3: Comparison of the round nozzle and the top nozzle

The enclosing of the weld seam minimizes the heat loss and allows a better control of the hot gas flow. Therefore, the polymer is heated more homogeneously and a better temperature distribution inside the polymer can be observed. This behavior has been investigated and confirmed by a large number of simulations, which will be shown in this article, and welding tests with plates of various thicknesses and burst pressure specimens. [25, 26, 28, 34]

In previous studies it was shown, that for polyamides with different base polymers and different glass fibre contents, a reduction in average heating time of 50 % is possible while the weld strength achieved is comparable or higher compared to the round nozzle system [25, 26, 28, 34]. This could be mainly explained by the uniform melting of the welding joint and the simultaneous absence of overheating and decomposing the polymer [35, 36].

6 VARIATION OF THE OPERATING CONDITIONS

The simulations are used for a comparison of the two nozzle systems, but since the focus is on the development of the top nozzle, the round nozzle is not discussed further in this article. All further investigations in this article are performed in the case of the top nozzle as this nozzle system shows the superior performance. The influences of different process parameters are investigated by simulations and temperature measurements with an IR camera system and thermocouples under variations of the materials and process parameters.

6.1 Simulations with variable heating times

Even with varying heating times (10.0 s, 12.5 s and 15.0 s), the simulation results for a PA6-GF40 and a PA66-GF35 are consistent with the temperatures measured during the welding process, Figure 14. The surface temperatures

measured by the IR camera are 21 K lower for PA6-GF40 and 20 K lower for PA66-GF35 than the temperature measured by the thermocouples at a heating time of 10.0 s, since the polymer cools down on the surface when the hot gas tool is removed. The temperatures of the thermocouples agree with the temperatures of the simulation results. At a heating time of 12.5 s and 15.0 s, the temperatures of the thermocouples, the IR camera system and the simulation are all in good agreement with each other.

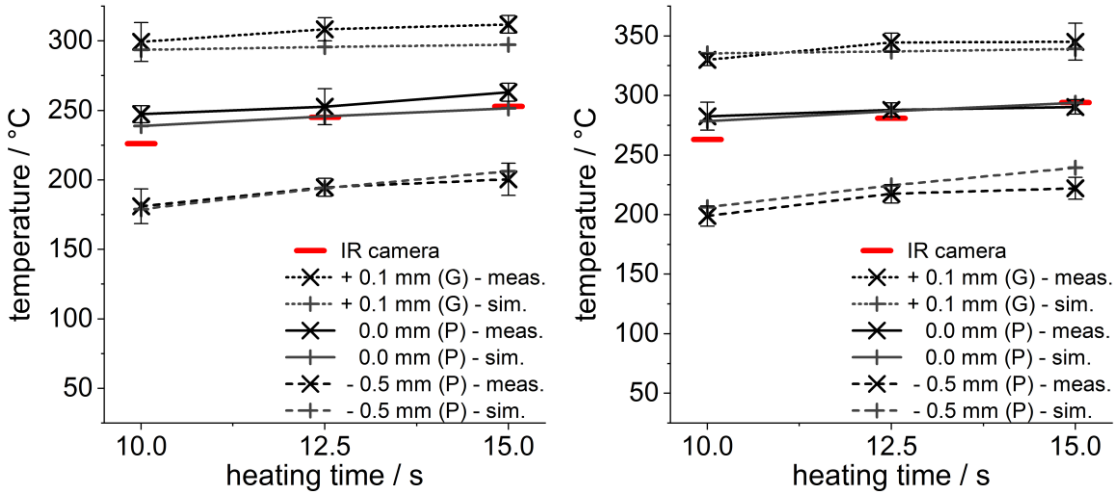

Figure 14: Comparison of measured (IR and thermocouple) and simulated temperature using a top nozzle at varying heating times; left: gas temperature of 300 °C on a PA6-GF40; right: gas temperature of 355 °C on a PA66-GF35

Please note that the next three figures compare the process behavior of the two materials PA6-GF40 and PA66-GF35. For this purpose, the temperature scale of the diagrams is adjusted according to the gas temperatures used. The melting points of the two materials are 220 °C (PA6-GF40) and 263 °C (PA66-GF35), as described in chapter 4.2. The polymer surface temperature and thus the temperatures inside the polymer increase due to longer heating times, Figure 15. A strong temperature drop can be observed between the gas temperature, the temperature on the polymer surface and the temperature inside the polymer. With longer heating times the difference between the polymer temperatures and the gas temperature decreases.

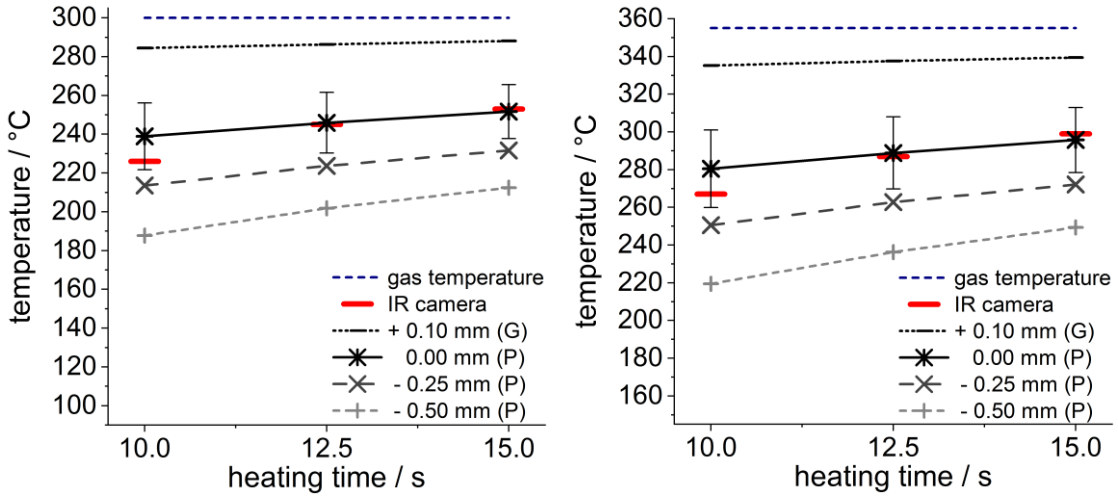

Figure 15: Influence of the heating time at a gas temperature of 300 °C (PA6-GF40 - left) and a gas temperature of 355 °C (PA66-GF35 – right)

6.2 Simulations with variable gas temperatures

The simulations for PA6-GF40 show that the temperatures arising at the polymer surface and in the polymer increase accordingly with higher gas temperatures, Figure 16. The same behavior can be observed for PA66-GF35, Figure 16.

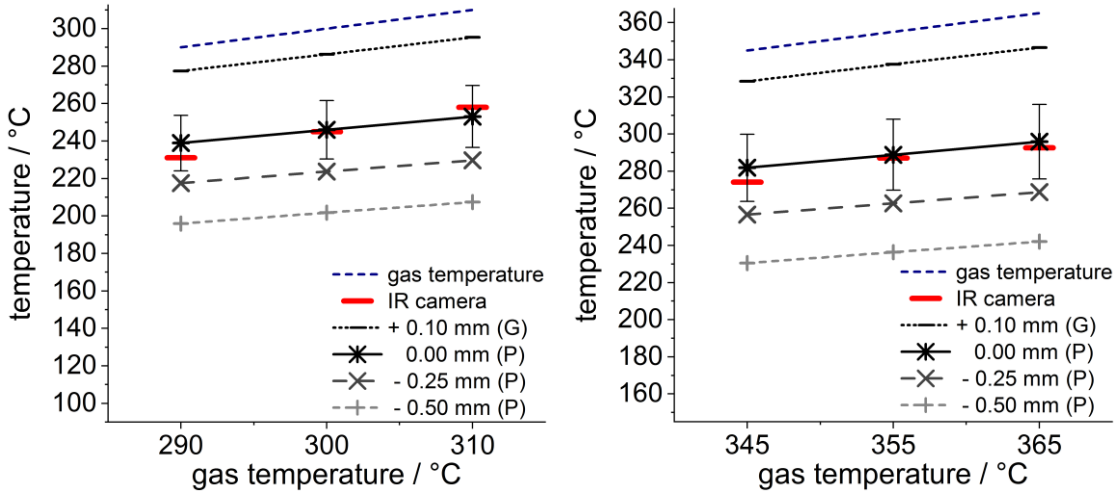

Figure 16: Dependence of polymer temperatures on gas temperature at 12.5 s heating time for PA6-GF40 (left) and PA66-GF35 (right)

The simulated temperatures arising at the polymer surface and in the polymer increase with higher gas temperatures. The simulated temperatures of the pol-

ymer surface are comparable to the temperatures measured by the IR camera system. A linear dependence of the temperatures of the polymer on the gas temperature can be observed. This seems to be reliable due to the almost constant values of the heat transfer coefficient and heat capacity of the polymer and of the nitrogen in the studied temperature range.

6.3 Simulations with variable volume flow rates

An increase of the volume flow rate leads to higher temperatures at the surface and in the polymer for PA6-GF40 and PA66-GF35, Figure 17. The simulated temperatures at the polymer surface agree with the temperatures measured with the IR camera system quite well. The minor variation of the heat transfer coefficient and of the heat capacity of the polymer with temperature results in a nearly linear dependence of the temperatures on the volume flow rate for the investigated conditions.

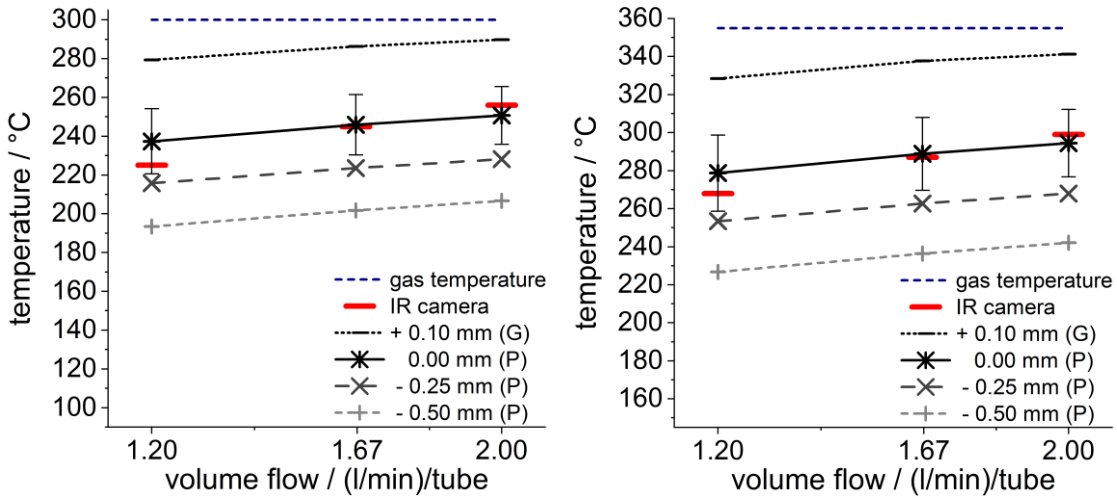

Figure 17: Influence of the volume flow rate at a gas temperature of 300 °C (PA6-GF40 - left) and a gas temperature of 355 °C (PA66-GF35 – right) with a heating time of 12.5 s

Conclusively, the simulations provides reliable results for the investigated polyamides at different gas temperatures and heating times. The simulations show that an increase in the process parameters gas temperature, heating time or volume flowrate lead to correspondingly higher polymer temperatures.

7 VARIATION OF GEOMETRICAL PARAMETERS

The manufacturing of hot gas tools with varied geometrical parameters is very complex and expensive. Therefore, the further investigations of the influence of various geometric parameters are performed using validated simulation. Four geometric parameters are varied to investigate their influence, Figure 18.

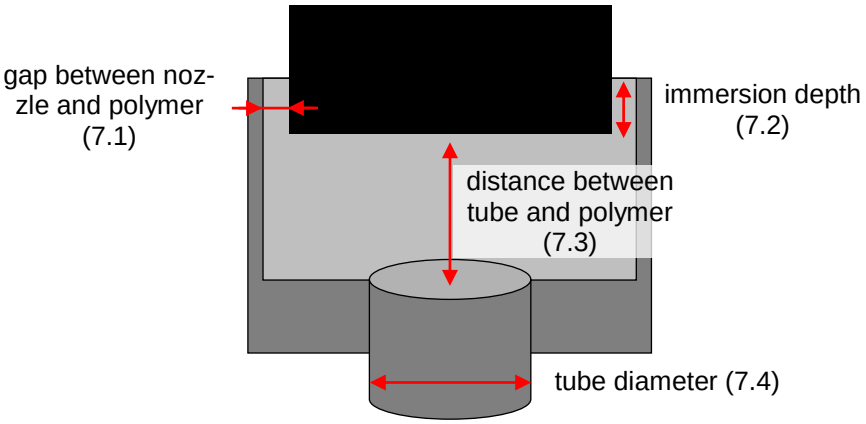

Figure 18: Sketch with the geometric parameters varied in the simulation

7.1 Influence of the gap between nozzle and polymer

The variation of the gap between polymer and top nozzle between 0.5 mm and 2.0 mm shows that a gap of 0.5 mm leads to the highest temperatures on and in the polymer, Figure 19. The temperature range on the polymer surface (0.00 mm) with a 0.5 mm gap (26 K) is larger compared to 1.0 mm gap (22 K). The temperature range is the difference between the highest and lowest simulated temperature at the surface of the polymer. A gap of more than 1.0 mm between the polymer and the top nozzle leads to a drop in average temperature of 12 K on the polymer surface from 291 °C to 279 °C. Inside the polymer, the temperature drops by 10 K each time the gap is increased by 0.5 mm. However, a gap smaller than 1.0 mm does not make sense for process-related reasons. Because, a gap smaller than 1.0 mm reduces the possibility of compensating for tolerance-related variations in the dimensions of the plastic components.

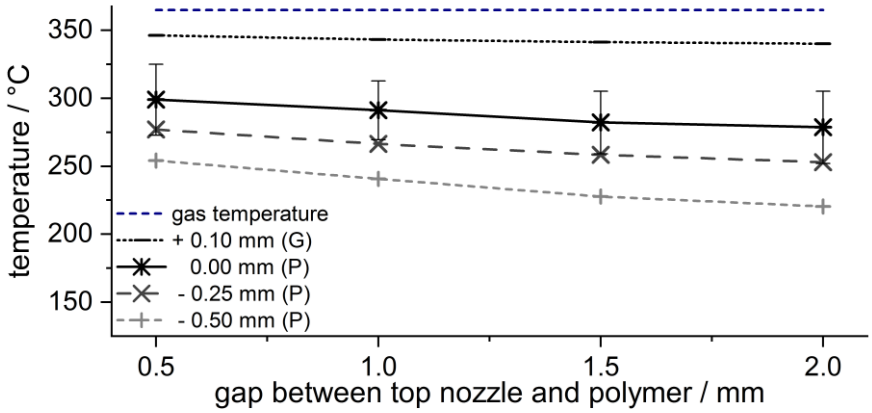

Figure 19: Influence of the gap between nozzle and polymer with 365 °C gas temperature, 12.5 s heating time and 1.67 l/min / tube nitrogen for PA66-GF35; (error bars indicate the temperature range)

7.2 Influence of the immersion depth

The variation of the immersion depth of the polymer into the top nozzle between - 2.0 mm and 0.5 mm shows that an immersion depth lower than - 0.5 mm leads to the highest temperatures on the surface and inside the polymer. If the polymer is not immersed into the top nozzle (immersion depth ≥ 0.0 mm), the temperatures on the surface of the polymer drop by 15 K. Therefore, it can be concluded that an immersion depth of - 0.5 mm is best, because a deeper immersion of the polymer does not lead to a better heating behavior and the sides of the joints are not melted without reason. An immersion depth of - 0.5 mm is also preferable, as weld seams on components are not always exposed.

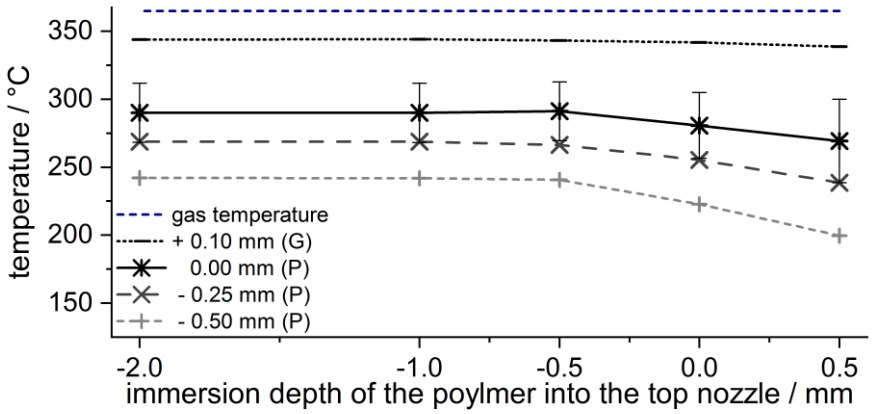

Figure 20: Influence of the immersion depth into the top nozzle with 365 °C gas temperature, 12.5 s heating time and 1.67 l/min / tube nitrogen for PA66-GF35; (error bars indicate the temperature range)

7.3 Influence of the distance between tube and polymer

Varying the distance between the nozzle opening of the top nozzle and the polymer surface between 2.0 mm and 6.0 mm shows that increasing the distance leads to slightly lower temperatures on the surface and inside the polymer, Figure 21. Overall, the distance between the nozzle opening and the polymer surface has no significant influence. However, a moderate distance is advisable for low-viscosity materials, since otherwise, the impact flow can cause forming crater-like structures on the polymer surface [25, 26]. For this reason, a distance of 4.5 mm between the round nozzle opening and the polymer surface is currently chosen.

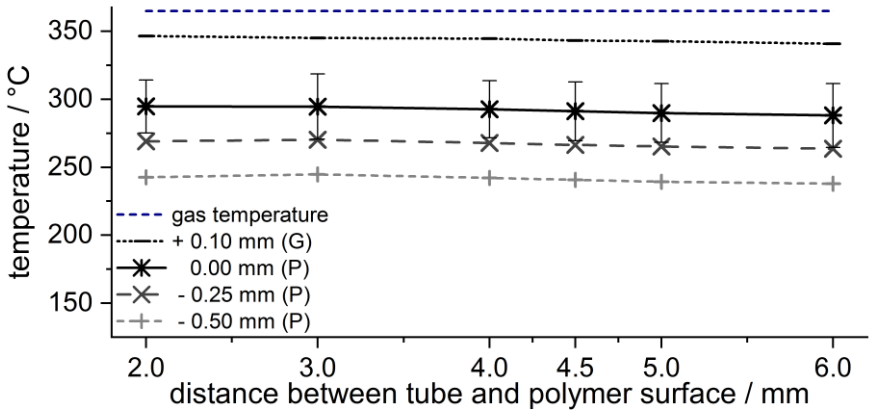

Figure 21: Influence of the distance between the tube in the top nozzle and polymer surface with 365 °C gas temperature, 12.5 s heating time and 1.67 l/min / tube nitrogen for PA66-GF35; (error bars indicate the temperature range)

7.4 Influence of the tube diameter

The simulation results of the variation of the tube diameter show that the temperatures on the surface and inside the polymer decrease with larger tube diameters, Figure 22. In addition, the temperature range increases with increasing tube diameters. A tube diameter of 1.2 mm or 1.5 mm leads to the highest temperatures on the surface and inside the polymer. Smaller tube diameters have higher flow velocity which can lead to crater-like structures on the surface of the polymer in case of low viscosity materials. Tube diameters of 1.7 mm or 2.0 mm lead to an efficient heating process with simultaneously low temperature ranges at the polymer surface. From a manufacturing point of view, increasing tube diameters make more sense, since this means lower manufacturing costs. The tube diameter depends mainly on the weld width of the part. For a 4 mm weld width a tube diameter of 1.7 mm or 2.0 mm is used. Smaller tube diameter are used for smaller weld width and larger tube diameter are used for larger weld width.

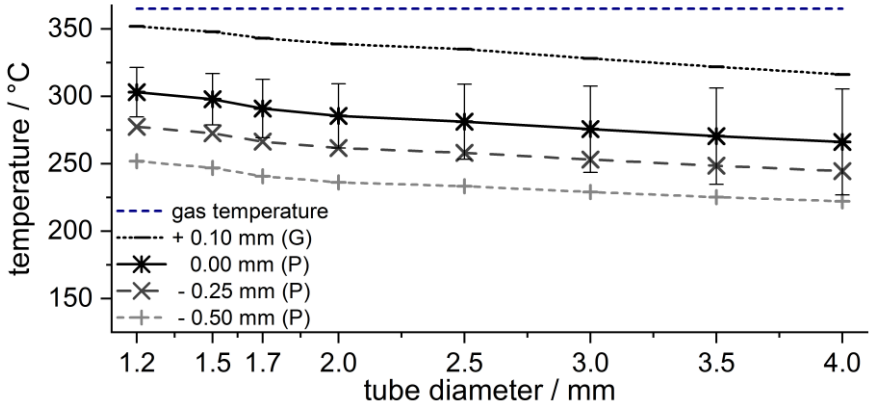

Figure 22: Influence of the tube diameter on the developing temperature with 365 °C gas temperature, 12.5 s heating time and 1.67 l/min / tube nitrogen for PA66-GF35; (error bars indicate the temperature range)

8 SUMMARY OF THE RESULTS AND OUTLOOK

Today hot gas welding processes often show limited processing windows and are therefore difficult to adjust and control. One reason for this is that by using the widely used round nozzle design the gas flow is difficult to control and thus the welding of the weld joint is less uniform. With the next generation top nozzle design the weld joint is entirely covered by the nozzle itself. As a result, the heat loss is minimized and the flow of the hot gas can be controlled much better. Therefore, the polymer is heated and melted more homogeneously and a better temperature distribution inside the polymer can be observed. This behavior has been investigated and confirmed by a large number of simulations and experimental results including temperature measurements.

The CFD simulations provide comparable results with the temperature measurements for two polyamides with different base polymers and different glass fiber content (PA6-GF40 and PA66-GF35) at varying heating times, temperatures of the hot gas tool and volume flows. The results of the simulations are validated by measurements with an IR camera system and lost thermocouples. Thus, the CFD simulation provides reliable results for the investigated polyamides at the studied gas temperatures, heating times and volume flows.

The simulations show that an increase in the process parameters gas temperature, heating time or volume flow leads to a correspondingly higher polymer temperature.

The geometrical variation of the gap distance between polymer and top nozzle shows that a smaller gap leads to higher temperatures on the surface and in-

side the polymer. A gap < 1.0 mm is not feasible for manufacturing reasons and leads primarily to the fact, that fewer tolerances can be compensated for the components to be welded. An immersion depth of - 0.5 mm into the polymer is recommendable, because a deeper immersion of the polymer does not lead to a better heating behavior and no immersion leads to a significant temperature drop inside the polymer. Varying the distance between the nozzle opening and the polymer surface shows that the distance between the nozzle opening and the polymer surface has no significant influence. However, a moderate distance is advisable for low-viscosity materials, since otherwise, the impact flow can cause crater-like structures to form on the polymer surface. The temperatures on the surface and inside the polymer decrease with larger tube diameters. Small tube diameters have the highest flow velocity which can lead to crater-like structures on the surface of the polymer in case of low viscosity materials.

The study of the geometrical parameters of the top nozzle indicates that tube diameters between 1.7 mm or 2.0 mm lead to an efficient heating process with simultaneously low temperature ranges in the polymer for a 4 mm wide weld seam. From a manufacturing point of view, larger tube diameters are preferable, since this means lower manufacturing costs. A gap of 1.0 mm between nozzle and polymer is recommendable and a distance of 4.5 mm is currently selected between the nozzle opening and the polymer surface.

From an economical point of view, the advantages of the new top nozzle design results in a reduced heating time and therefore a reduced welding cycle time as well as a reduced hot gas consumption. The wider process window and the shorter heating time of the top nozzle lead to greater reliability of the hot gas welding process [25, 26, 28, 34].

With the new top nozzle design, higher temperatures in the polymer are possible for polyamides with higher melting points like PA6T/XT (PPA) [26]. The target temperatures could be achieved in shorter heating times which reduce the thermal damage of the material. This enables the welding of new materials, which have a higher melting point. These new materials allow further application areas.

It could be shown that the CFD simulation of the hot gas welding process for plate-shaped components (2D welds) provides reliable results. In a further step, the CFD simulation could be applied to three-dimensional welds, e.g. inclined and curved welds. With the help of CFD simulations, the flow guidance within the hot gas welding tool can be optimized in the future and better tailored to the components to be welded. Furthermore, the shape of the top nozzle could be further investigated and improved if necessary.

9 ACKNOWLEDGEMENT

In the joint research project between GMB Kunststoffteile GmbH and Esslingen University of Applied Sciences on hot gas welding (funded by the “Zentrale Innovationsprogramm Mittelstand (ZIM)” from the Federal Ministry for Economic Affairs and Energy - funding code: ZF4166303FH8), the investigated new nozzle system – the top nozzle – has been develeoped [37].

All 3D simulations are performed on the bwUniCluster using STAR-CCM+. BwUniCluster is Baden-Württemberg´s general purpose tier 3 high performance computing cluster (HPC) within the bwHPC project. The authors acknowledge support by the state of Baden-Württemberg through bwHPC.

Literatur

[1]	Rattke, M.; Natrop, J.	Infrared heating in plastics welding technology Fügen von Kunststoffen - Joining Plastics (2007), pp. 58-63, DVS Media GmbH, Düsseldorf; ISSN 1864-3450
[2]	Fuhrich, R.; Gehde, M.	Contour-following infrared radiator for the welding of plastics with high time and energy efficiencies Fügen von Kunststoffen - Joining Plastics (2014), pp. 204-211, DVS Media GmbH, Düsseldorf; ISSN 1864-3450
[3]	Gehde, M.; Friedrich, S.; Mochev, S.	Radiant heating during plastics welding with infrared radiation Fügen von Kunststoffen - Joining Plastics (2008), pp. 58-63, DVS Media GmbH, Düsseldorf; ISSN 1864-3450
[4]	Fuhrich, R.; Gehde, M.; Friedrich, S.	Process temperature measurement in infrared welding Fügen von Kunststoffen - Joining Plastics (2011), pp. 34-39, DVS Media GmbH, Düsseldorf; ISSN 1864-3450
[5]	Schulz, J.-E.	Prozess- und Bauteiluntersuchungen zum Laserdurchstrahlschweißen von Kunststoffen Dissertation, RWTH Aachen, 2002
[6]	Klein, H. M.	Laserschweißen von Kunststoffen in der Mikrotechnik Dissertation, RWTH Aachen, 2001
[7]	Friedrich, S.	Lineares Vibrationsschweißen von Kunststoffen im industriellen Umfeld. Einflüsse und Restriktionen Dissertation, Technische Universität Chemnitz, 2014
[8]	Schlarb, A.K.	Zum Vibrationsschweißen von Polymerwerkstoffen. Prozess-Struktur-Eigenschaften Dissertation, Universität Essen, 1989
[9]	Mochev, S.; Endemann, U. M.	Mehr als nur heiße Luft: Systematische Prozessoptimierung für das Heißgasschweißen Kunststoffe (2016) 12, pp. 76-79, Carl Hanser Verlag, München; www.kunststoffe.de/2124277

[10]	Rattke, M.; Natrop, J.	Newly developed convection welding process on a natural gas basis Fügen von Kunststoffen - Joining Plastics (2008), pp. 129-133, DVS Media GmbH, Düsseldorf; ISSN 1864-3450
[11]	Barkhoff, R.; Happel, J.	Quadralux: Hybrid heating procedure for the welding of plastics Fügen von Kunststoffen - Joining Plastics (2019), pp. 161, DVS Media GmbH, Düsseldorf; ISSN 1864-3450
[12]	Belmann, A.	Reducing contaminations during the joining of plastics Fügen von Kunststoffen - Joining Plastics (2017), pp. 34-41, DVS Media GmbH, Düsseldorf; ISSN 1864-3450
[13]	Potente, H.; Schöpper, V.; Hoffschlag, R.	Investigations into the melt adhesion during heated tool welding Fügen von Kunststoffen - Joining Plastics (2010), pp. 102-107, DVS Media GmbH, Düsseldorf; ISSN 1864-3450
[14]	Egen, U.	Gefügestruktur in Heizelementschweißnähten an Polypropylen-Rohren Dissertation, Universität Kassel 1985
[15]	Kreiter, J.	Optimierung der Schweißnahtfestigkeit von Heizelementstumpfschweißungen von Formteilen durch verbesserte Prozessführung und Selbsteinstellung Dissertation, Universität Paderborn 1987
[16]	Bonten, C.	Beitrag zur Erklärung des Wirkmechanismus in Schweißverbindungen aus teilkristallinen Thermoplasten Dissertation, Universität Essen 1998
[17]	Baudrit, B.; et al.	Energy efficiency during heated tool welding Fügen von Kunststoffen - Joining Plastics (2014), pp. 197-203, DVS Media GmbH, Düsseldorf; ISSN 1864-3450

[18]	Potente, H.,; Schöppner, V.; et al.	Saving cycly time by means of intensive cooling during heated tool welding Fügen von Kunststoffen - Joining Plastics (2008), pp. 50-56, DVS Media GmbH, Düsseldorf; ISSN 1864-3450
[19]	Friedrich, N.; Schöppner, V.	Reducing the cycle time in heated tool welding without any loss in quality as a result of forced cooling using compressed air Fügen von Kunststoffen - Joining Plastics (2012), pp. 134-141, DVS Media GmbH, Düsseldorf; ISSN 1864-3450
[20]	Mochev, S.	Heißgasschweißen – Aktuelle Entwicklungen und Möglichkeiten Fachtagung: Fügen von Kunststoffen im Automobil, 06.-07.06.2018, Landshut, Carl Hanser Verlag, München
[21]	Deckert, M. H.; Schmid, J.; Weißer, D.	Neuartiges Heißgasschweißen von Kunststoffbauteilen Spektrum 48 – Hochschule Esslingen, pp. 21-23, ISSN 1864-0133
[22]	Rzepka, G.	Feste Verbindung unter besonderer Atmosphäre. Wie partikelarmes, berührungsloses Schweißen von technischen bis hin zu Hochleistungskunststoffen gelingt K-Profi (2021), pp. 32-37, ISSN 2195-2434
[23]	Mochev, S.; Endemann, U. M.;	Faster and Better Welding: Tools Adaption Reduces Process Times and Improves Weld Quality Kunststoffe international (2018) 9, pp. 57-59, Carl Hanser Verlag, München, www.kunststoffe.de/6708650
[24]	Bialaschik, M.; Schöppner, V.; et al.	Influence of material degradation on weld seam quality in hot gas butt welding of polyamides Welding in the World (2021) 65, pp. 1161–1169, DOI: 10.1007/s40194-021-01108-0
[25]	Schmid, J.; Deckert, M. H.; et al.	Reduktion der Erwärmungszeit beim Heißgasschweißen Zeitschrift Kunststofftechnik 17 (2021), pp. 112–128, DOI: 10.3139/O999.03022021

[26]	Schmid, J.; Deckert, M. H.; et al.	Heißgasschweißen in der Komfortzone - Neuartige Düsengeneration eröffnet vielfältige Möglichkeiten Zeitschrift Kunststoffe (2021), pp. 80–82, www.kunststoffe.de/a/ausgabe/ausgabe-092021-344568
[27]	Albrecht, M.; Bialaschik, M. O.; et al.	Hot gas welding – Influences of the tool Design, AIP Conference Proceedings 2289 (2020), DOI: 10.1063/5.0029478
[28]	Schmid, J.; Deckert, M. H.; et al.	Increase of the efficiency in hot gas welding by optimization of the gas flow Technologies for Lightweight Structures 5(1) (2021), Special issue: 5th International MERGE Technologies Conference (IMCT), Chemnitz 2021, pp. 32-40 DOI: 10.21935/tls.v5i1.154
[29]	Albrecht, M.; Bialaschik, M. O.; et al.	Hot gas butt welding of plastics Fügen von Kunststoffen - Joining Plastics 15 (2021), pp. 162-169, DVS Media GmbH, Düsseldorf, ISSN 1864-3450
[30]	VDI	VDI Wärmeatlas DOI: 10.1007/978-3-642-19981-3
[31]	Gordon, R.; Akfirat, J. C.	The role of turbulence in determining the heat-transfer characteristics of impinging jets. Int. J. Heat Mass Transf. 8 (1965), pp. 1261–1272 DOI: 10.1016/0017-9310(65)90054-2
[32]	Simionescu, Ş.-M.; et al.	Impinging Air Jets on Flat Surfaces at Low Reynolds Numbers Energy Procedia 112 (2017), pp. 194–203 DOI: 10.1016/j.egypro.2017.03.1083
[33]	Lanxess Deutschland GmbH	Die Zwillinge unter den Polyamiden. Eigenschaftsvergleich PA6 und PA66 Technische Information – Lanxess Deutschland GmbH (2009)
[34]	Schmid, J.; Deckert, M. H.; et al.	Reduktion der Erwärmungszeit beim Heißgasschweißen. Technomer 2021. 27. Fachtagung über Verarbeitung und Anwendung von Polymeren. Chemnitz 2021

DOI: 10.3139/O999.03022021

[35] Pongratz, S. Alterung von Kunststoffen während der Verarbeitung und im Gebrauch

Dissertation, Universität Erlangen-Nürnberg 2000

[36] Ehrenstein, G.W.; Pongratz, S. Beständigkeit von Kunststoffen

Carl Hanser Verlag, München 2007

DOI: 10.3139/9783446411494

[37] Böhler, G.; Böhler, S. DE 20 2021 101 884 U1 – Gebrauchsmusterschrift: Vorrichtung zum Schweißen von Kunststoffteilen. GMB Kunststoffteile GmbH, Pleidelsheim 2020

Bibliography

DOI 10.3139/O999.01032022
Zeitschrift Kunststofftechnik / Journal of Plastics Technology 18 (2022) 3; page 117–145

ISSN 1864 – 2217

Stichworte:
Heißgasschweißen, Kunststoffschweißen, CFD-Simulation, Düsen, Erwärmen des Kunststoffes

Keywords:
hot gas welding, plastic welding, CFD simulation, nozzle, heating of the polymer

Autor / author:
Johannes Schmid, M.Sc.[1]
Dennis F. Weißer, M.Sc.[1]
Dennis Mayer, M.Eng.[1]
Prof. Dr.-Ing. habil. Lothar Kroll[2]
Dr.-Ing. Sascha Müller[2]
Prof. Dr.-Ing. Rainer Stauch[1]
Prof. Dr.-Ing. Matthias H. Deckert[1]
[1]Fakultät für Maschinen und Systeme, Hochschule Esslingen
[2]Professur für Strukturleichtbau und Kunststoffverarbeitung, Technische Universität Chemnitz

E-Mail: johannes.schmid@hs-esslingen.de
Webseite: www.hs-esslingen.de